AEM
Journals.ASM.org

Novel pH-Stable Glycoside Hydrolase Family 3 β-Xylosidase from *Talaromyces amestolkiae*: an Enzyme Displaying Regioselective Transxylosylation

Manuel Nieto-Domínguez, Laura I. de Eugenio, Jorge Barriuso, Alicia Prieto, Beatriz Fernández de Toro, Ángeles Canales-Mayordomo, María Jesús Martínez

Centro de Investigaciones Biológicas (CIB), CSIC, Madrid, Spain

This paper reports on a novel β-xylosidase from the hemicellulolytic fungus *Talaromyces amestolkiae*. The expression of this enzyme, called BxTW1, could be induced by beechwood xylan and was purified as a glycoprotein from culture supernatants. We characterized the gene encoding this enzyme as an intronless gene belonging to the glycoside hydrolase gene family 3 (GH3). BxTW1 exhibited transxylosylation activity in a regioselective way. This feature would allow the synthesis of oligosaccharides or other compounds not available from natural sources, such as alkyl glycosides displaying antimicrobial or surfactant properties. Regioselective transxylosylation, an uncommon combination, makes the synthesis reproducible, which is desirable for its potential industrial application. BxTW1 showed high pH stability and Cu^{2+} tolerance. The enzyme displayed a pI of 7.6, a molecular mass around 200 kDa in its active dimeric form, and K_m and V_{max} values of 0.17 mM and 52.0 U/mg, respectively, using commercial *p*-nitrophenyl-β-D-xylopyranoside as the substrate. The catalytic efficiencies for the hydrolysis of xylooligosaccharides were remarkably high, making it suitable for different applications in food and bioenergy industries.

Plant biomass represents the most abundant renewable energy resource available on earth. It is composed mainly of cellulose and hemicellulose, two polysaccharides that constitute the raw material for the so-called second-generation (2G) bioethanol industry. The production of this biofuel has received special attention in recent years because it is based on the use of nonfood sources of cellulosic biomass (1). It has been pointed out that energy crops should be restricted to metal-contaminated soils in order to avoid cultivation competition against the food industry (2, 3).

In order to make the production of this biofuel economically viable, many modifications have been introduced into the industrial process in recent years. Among them, the strategy of combining enzymatic hydrolysis of lignocellulose with ethanol fermentation in a single process known as simultaneous saccharification and fermentation (SSF) is a significant step forward, but reduced production costs and improved yields are still necessary (1). Most studies have been using agricultural wastes as raw materials, usually after a physicochemical pretreatment to disrupt the lignocellulose structure to enhance cellulose and hemicellulose accessibility. Nevertheless, the industrial procedure currently used to produce 2G ethanol consists of fermenting glucose, which is enzymatically released from cellulose by using *Saccharomyces cerevisiae* as a biocatalyst (4). To increase process yields, hemicellulose hydrolysis and pentose fermentation are extremely relevant. Within this heterogeneous group of polysaccharides, xylans are most abundant in hardwoods and grass. They are composed of a backbone of β-1,4-linked D-xylopyranosyl units highly substituted with arabinofuranose, glucose, glucuronic or *methyl*-glucuronic acid, and acetyl side groups. The enzymatic conversion of xylans into xylose at the industrial level is crucial to improve the biomass conversion yield, although this aspect requires further development (5). Due to the complexity and heterogeneity of xylans, their complete breakdown requires the coordinated actions of several hydrolases, among which endo-β-1,4-xylanases (EC 3.2.1.8) and β-xylosidases (EC 3.2.1.37) play important roles. The first enzymes cut the xylan backbone into soluble oligosaccharides that can be depolymerized to xylose by the action of β-xylosidases. There is much interest in identifying novel β-xylosidases, since robust enzymes are needed for lignocellulose biomass applications. In fact, most of the commercial enzymatic preparations are deficient in this glycosyl hydrolase activity (6).

Hemicellulases can also be used in many other industrial areas. For example, a complete biodegradation of xylans is one of the goals for the paper industry, since it would improve the biobleaching process and hence reduce chlorine use. In the animal feed area, β-xylosidase and other lignocellulolytic enzymes can be added to animal feed in order to speed weight gain in animals. Endoxylanases and β-xylosidases hydrolyze hemicelluloses in cereals, facilitating the mobility of nutrients and promoting their absorption (7).

β-Xylosidases catalyze the hydrolysis of the glycosidic linkage by two possible mechanisms. In the single-displacement mechanism, a water molecule directly breaks the bond, while the double-displacement mechanism implies the formation of an enzyme-

Received 26 May 2015 **Accepted** 1 July 2015

Accepted manuscript posted online 6 July 2015

Citation Nieto-Domínguez M, de Eugenio LI, Barriuso J, Prieto A, Fernandez de Toro B, Canales-Mayordomo A, Martínez MJ. 2015. Novel pH-stable glycoside hydrolase family 3 β-xylosidase from *Talaromyces amestolkiae*: an enzyme displaying regioselective transxylosylation. Appl Environ Microbiol 81:6380–6392. doi:10.1128/AEM.01744-15.

Editor: D. Cullen

Address correspondence to María Jesús Martínez, mjmartinez@cib.csic.es.

Supplemental material for this article may be found at http://dx.doi.org/10.1128/AEM.01744-15.

doi:10.1128/AEM.01744-15

substrate intermediate. In the first case, the released xylose suffers inversion of its anomeric configuration, while the β configuration is kept if the second mechanism occurs (8). According to the Carbohydrate Active enZymes database (CAZy; http://www.cazy.org/), fungal β-xylosidases belong to three families: glycoside hydrolase family 3 (GH3), GH43, and GH54. Family GH43 includes hydrolases with the inverting mechanism, while families GH3 and GH54 include β-xylosidases with a retaining mechanism. Many retaining β-xylosidases are capable of catalyzing the formation of a new glycosidic linkage, transferring a xylosyl residue from a donor to an alcohol group of a particular acceptor in a process called transxylosylation. This type of activity is especially interesting because this mechanism allows the synthesis of conventional as well as new xylooligosaccharides (XOs) of different degrees of polymerization (DP) with a potential outlet in prebiotics and interest for pharmacological applications (9). As an example, novel glycosidic-polyphenolic antioxidants with greater solubility and bioavailability can be synthesized in such reactions (10).

Many cellulolytic and hemicellulolytic fungi belonging to the phylum Ascomycota have been described. Although *Aspergillus* and *Trichoderma* species have been the most extensively studied, *Penicillium* strains seem to be good candidates as sources of lignocellulolytic enzymes (11). In a previous study, a perfect state (determined when fungal sexual phase is observed) of a *Penicillium* species, later identified as *Talaromyces amestolkiae*, was selected for secreting a large amount of cellulases and hemicellulases (12).

This work reports the production, isolation, and biochemical characterization of a β-xylosidase from *T. amestolkiae*. In addition, the sequencing and molecular characterization of the new enzyme are presented and its potential use in hydrolysis and regioselective transxylosylation reactions is discussed.

MATERIALS AND METHODS

Fungal strain and culture media. The *T. amestolkiae* strain was isolated from cereal waste and deposited in the IJFM culture collection of the Centro de Investigaciones Biológicas (Madrid, Spain) with the reference designation A795.

Sporulation took place after the fungus was cultured on 2% agar-malt petri dishes at 26 to 28°C for 7 days. About 1 cm^2 of agar-malt with growing mycelium was cut and added to a 5-ml solution of 1% NaCl and 0.1% Tween 80. The mixture was shaken, and 200 μl was used to inoculate 250-ml flasks with 50 ml of CSS medium, containing the following (liter^{-1}): 40 g glucose, 0.4 g $FeSO_4 \cdot 7H_2O$, 9 g $(NH_4)_2SO_4$, 4 g K_2HPO_4, 26.3 g corn steep solid, 7 g $CaCO_3$, and 2.8 ml soybean oil. pH was adjusted to 5.6, and the culture was incubated at 28°C and 180 rpm for 5 days.

β-Xylosidase production was carried out in 250-ml flasks with 50 ml of Mandels medium and 2 ml of the CSS culture prepared for inoculum. Mandels medium contained the following (liter^{-1}): 2.0 g KH_2PO_4, 1.3 g $(NH_4)_2SO_4$, 0.3 g urea, 0.3 g $MgSO_4 \cdot 7H_2O$, 0.3 g $CaCl_2$, 5 mg $FeSO_4 \cdot 7H_2O$, 1.6 mg $MnSO_4 \cdot H_2O$, 1.4 mg $ZnSO_4 \cdot 7H_2O$, and 1 g Bacto peptone (pH 4.5). Mandels medium was supplemented with 2% beechwood xylan (≥90% xylose), provided by Sigma-Aldrich, as the carbon source and β-xylosidase inducer. Beechwood xylan is a hardwood xylan with a backbone of β-1,4-linked D-xylopyranosyl residues. Branches are composed mainly of 4-*O*-methylglucuronic acid attached to xylose at the C-2 position and acetyl groups at the C-2 or C-3 position (13). In some experiments, 1% xylan, 3% xylan, 1% D-xylose, 1% D-glucose, or 1% Avicel (Merck) was used as an alternative carbon source. Cultures were incubated at 28°C and 180 rpm, and samples were periodically withdrawn from three replicate flasks and centrifuged at 20,000 × *g* for 5 min to separate the culture liquids from the mycelium.

Enzyme and protein assays. β-Xylosidase activity was measured spectrophotometrically by the release of 4-nitrophenol (*p*NP) (ε_{410} = 15,200 M^{-1} cm^{-1}) from *p*-nitrophenyl-β-D-xylopyranoside (*p*NPX) (Sigma-Aldrich). The standard reaction mixture consisted of 3.5 mM *p*NPX, 50 mM sodium citrate buffer (pH 5), 0.1% bovine serum albumin (BSA), and the appropriate dilution of the purified enzyme or culture crude extract. Standard assays were incubated at 50°C and 500 rpm for 5 and 10 min, in order to check the linearity of the measured activity, and the reactions were stopped by the addition of 500 μl 2% Na_2CO_3. Bovine serum albumin was added for stability issues. One unit of β-xylosidase activity was defined as the amount of enzyme that hydrolyzes 1 μmol of *p*NPX per minute.

Direct quantification of released xylose was performed either by gas chromatography-mass spectrometry (GC-MS) or spectrophotometrically, the latter using standards and reagents of the D-xylose assay kit (Megazyme) and in accordance with the manufacturer's instructions. For GC-MS analysis, xylose was previously converted into its alditol acetate derivative as described by Notararigo et al. (14). Sample components were separately injected for identification on the basis of their retention time. Depending on the reactions, inositol or galactosamine was used as the internal standard, to avoid overlapping with the reaction products. The D-xylose assay kit method is based on the complete conversion of free xylose into its beta anomer and then into D-xylonic acid, releasing NADH. The xylose concentration was determined by monitoring NADH absorbance at 340 nm.

Hydrolytic activity against glucose-containing substrates was measured by quantifying free glucose after the enzymatic reactions. The measurement was carried out colorimetrically through the coupling of glucose oxidase and peroxidase reactions using a Glucose-TR kit (Spinreact).

Proteins were quantified by the bicinchoninic acid (BCA) method, using Pierce reagents and bovine serum albumin as the standard, according to the manufacturer's instructions.

β-Xylosidase purification. β-Xylosidase production was carried out by culturing *T. amestolkiae* in 250-ml flasks with 50 ml of Mandels medium and 2% beechwood xylan as described above. Three-day-old cultures were harvested by filtration through filter paper in order to separate mycelium from culture liquids. The filtrate was centrifuged at 10,000 × *g* and 4°C for 30 min, and the supernatant was filtered through 0.8-, 0.45-, and 0.22-μm disc filters (Merck-Millipore). Finally, the crude was concentrated and dialyzed against 10 mM acetate buffer (pH 4) using a 5-kDa cutoff membrane.

β-Xylosidase was purified after three chromatographic steps using an ÄKTA Purifier chromatography system (GE Healthcare). The dialyzed crude enzyme was loaded onto a 5-ml HiTrap SPFF cartridge (GE Healthcare), equilibrated in 10 mM sodium acetate buffer (pH 4). The bound proteins were eluted with a linear gradient of 1 M NaCl from 0 to 50% in 25 ml at a flow rate of 1 ml/min. The column was then washed with 1 M NaCl (10 ml) and allowed to reequilibrate with the starting buffer for 10 min. Fractions with β-xylosidase activity were collected, desalted using PD-10 columns (GE Healthcare) equilibrated with 10 mM sodium acetate buffer (pH 4), and applied to a 1-ml Mono S 5/50 GL column (GE Healthcare) previously equilibrated in the same buffer. Proteins were eluted with a linear gradient of 1 M NaCl from 0 to 40% in 25 ml at a flow rate of 1 ml/min. The column was washed with 1 M NaCl (5 ml) and reequilibrated to the starting conditions for 5 min. Fractions with β-xylosidase activity were collected, mixed, dialyzed, and concentrated by ultrafiltration using Amicon Ultra-15 centrifugal devices (5-kDa cutoff; Merck-Millipore). Finally, samples were applied onto a Superose 12 HR 10/30 column (GE Healthcare) equilibrated and eluted with the same buffer with 100 mM NaCl at a flow rate of 0.5 ml/min for 50 min. The purified enzyme was concentrated by ultrafiltration (5-kDa cutoff; Merck-Millipore) and stored at 4°C. The isolated β-xylosidase was named BxTW1.

Physicochemical properties. The molecular mass of BxTW1 was estimated by SDS-PAGE (7.5% acrylamide) gels using Precision Plus protein dual color standards (Bio-Rad), and proteins were stained with Coomassie brilliant blue R-250 (Sigma-Aldrich). The molecular mass of the

purified protein was also calculated by size-exclusion chromatography on a Superose 12 HR 10/30 column previously calibrated with a standard protein kit (GE Healthcare) containing chymotrypsinogen A (19.5 kDa), ovalbumin (48.2 kDa), BSA (73.5 kDa), aldolase (170 kDa), and ferritin (460 kDa). Calibrants and samples were analyzed as described above. The accurate molecular mass and homogeneity of the pure enzyme were established by matrix-assisted laser desorption ionization–time of flight mass spectrometry (MALDI-TOF) using an Autoflex III instrument (Bruker Daltonics).

The isoelectric point of the protein was determined by isoelectrofocusing in 5% polyacrylamide gels using pH 3 to 10 ampholytes (GE Healthcare), with 1 M H_3PO_4 and 1 M NaOH as anode and cathode buffers, respectively. The pH gradient was measured directly on the gel using a contact electrode (Crison). β-Xylosidase activity was detected after incubation of the gels with 40 μM *p*-methylumbelliferyl β-D-xylopyranoside (Sigma-Aldrich) as described by Yan et al. (15), with *p*-methylumbelliferone fluorescence visualized under UV light by use of the Gel Doc XR+ system (Bio-Rad).

The coding DNA sequence of the enzyme was used to predict the theoretical pI and molecular mass of the protein. To do so, it was first converted into an amino acid sequence using the ExPASy Bioinformatics Resource Portal; this sequence was then submitted to the SignalP 4.1 server for identifying and locating the signal peptide, which was excluded from the mass prediction. Then, the mature protein sequence was analyzed using the Compute pI/M_w tool of the ExPASy Bioinformatics Resource Portal. The information was also submitted to the Eukaryotic Linear Motif resource (http://elm.eu.org/) in order to search for predicted posttranslational modification sites. The following parameters were selected: cell compartment, extracellular; taxonomic content, *T. amestolkiae*; motif probability cutoff, 100.

The N-carbohydrate content of β-xylosidase was demonstrated by the difference between the protein molecular mass before and after treatment with endoglycosidase H (Endo H; Roche), with both values estimated by SDS-PAGE in 7.5% polyacrylamide gels.

To determine the values of optimal temperature and pH, the ranges of temperature and pH stability, and the temperature at which the enzyme loses 50% activity after 10 min of incubation (T50) of the purified enzyme, the standard reaction mixtures contained 120 mU/ml of BxTW1 (4.0 μg protein/ml) and 0.1% BSA to ensure the validity of the results regardless of the enzyme concentration. The particular conditions for each experiment are described below.

The optimal temperature of BxTW1 was determined by incubating it at a temperature range of 30 to 70°C for 5 and 10 min. The optimal pH was determined using a pH range from 2.2 to 9 at 50°C for 10 min. In order to adjust pH values, the sodium citrate buffer of the standard reaction mixture was replaced by the one appropriate for each segment of the range: glycinate (pH 2.2 to 3), formate (pH 3 or 4), acetate (pH 4 to 5.5), phosphate (pH 5.5 to 7).

The T50 value, defined as the temperature at which the enzyme loses 50% activity after 10 min of incubation, was determined by heating the protein at a range of temperatures from 45 to 75°C, cooling at 4°C for 10 min, and rewarming to room temperature for 5 min before measuring the residual activity by the standard assay. The temperature at which the enzyme retained the maximum residual activity was taken as 100%.

β-Xylosidase thermostability was studied by incubating the purified enzyme in 10 mM sodium acetate buffer (pH 4) for 72 h at temperatures ranging from 30 to 70°C. Samples were collected at different times, and residual activity was assayed under standard conditions. pH stability was analyzed in a range from 2.2 to 9 by incubating the samples at 4°C for 72 h. In both assays, 100% corresponds to the initial activity.

The effect of common chemical compounds on β-xylosidase activity was studied by adding them to the reaction mixture. LiCl, KCl, $AgNO_3$, $MgSO_4$, $CaCl_2$, $BaCl_2$, $MnCl_2$, $FeSO_4$, $CoCl_2$, $NiSO_4$, $CuSO_4$, $ZnSO_4$, $HgCl_2$, $Pb(NO_3)_2$, $AlNH_4(SO_4)_2$, $FeCl_3$, and EDTA were assayed at a final concentration of 5 mM, while 2-mercaptoethanol (2-ME) and dithiothreitol (DTT) were added at a final concentration of 10 mM. The assay was carried out under standard conditions and in 50 mM sodium acetate (pH 5) to test the impact of the mild chelating effect described for sodium citrate (16).

Substrate specificity. The activity of pure BxTW1 was tested against the nitrophenyl substrates *p*NPX, *p*-NP-α-L-arabinopyranoside, *p*-NP-α-L-arabinofuranoside, *p*-NP-β-D-glucopyranoside, *o*-NP-β-D-glucopyranoside, *p*-NP-α-D-glucopyranoside, *p*-NP-α-L-rhamnopyranoside, *p*-NP-β-D-galactopyranoside, and *p*-NP-β-D-fucopyranoside (Sigma-Aldrich), at a final concentration of 3.5 mM. The activity of the enzyme was also assayed using as substrates (in 20 mM concentrations) the xylooligosaccharides xylobiose (X2), xylotriose (X3), xylotetraose (X4), xylopentaose (X5), and xylohexaose (X6) (Megazyme) and the disaccharides lactose, maltose, sucrose, lactose, gentiobiose, and cellobiose (Sigma-Aldrich). Finally, the catalytic activity of BxTW1 against polysaccharides was evaluated using 20 mg/ml of beechwood xylan and laminarin from *Laminaria digitata* (Sigma-Aldrich). The assays were carried out under standard conditions, and activity was measured by quantification of the released nitrophenol in the case of nitrophenyl substrates, xylose for xylooligosaccharides and beechwood xylan, and glucose for disaccharides and laminarin. The concentrations of released xylose and glucose were measured by using the D-xylose assay kit and the Glucose-TR kit, respectively, as described above.

The kinetic parameters of BxTW1 for each specific substrate were determined by using increasing substrate concentrations in a range from 0.078 to 20 mM. The experimental data derived from hydrolysis of *p*NPX, *p*NPAra, xylobiose, xylotriose, xylotetraose, xylopentaose, xylohexaose, and beechwood xylan were adjusted by least-squares to the Lineweaver-Burk linear equation of the Michaelis-Menten model. One unit of activity against XOS was defined as the amount of enzyme that totally hydrolyzed 1 μmol of the selected XOS to xylose per minute. Product inhibition by xylose was also studied, and K_i was determined against *p*NPX in the presence of 2.5, 5, and 10 mM xylose.

A more intensive study of BxTW1 behavior using xylotriose as the substrate was carried out by nuclear magnetic resonance (NMR) spectroscopy. The assay consisted of incubating 20 mM xylotriose with 800 mU/ml of BxTW1, expressed under standard conditions, in 50 mM formate buffer (pH 3) at 25°C. The concentrations of residual substrate and reaction products (disaccharide and monosaccharide) were monitored by acquiring ^{1}H-NMR spectra at different reaction times, until the complete conversion of xylotriose and xylobiose into xylose was detected. The amounts of each compound were compared by integrating distinctive signals: xylose was analyzed from H5 (δ 3.8), and xylotriose from H′5 (δ 4.03). Xylobiose lacked a specific signal in the ^{1}H-NMR spectrum, so it was quantified by subtracting xylotriose H′5 (δ 4.03) from H5 (δ 3.9), which overlaps the signals from xylobiose and xylotriose.

Transxylosylation reactions. The relationship between the initial rates of transxylosylation and the acceptor concentration was studied. Xylobiose and xylotriose in a range of concentrations from 1.25 to 80 mM were incubated with 200 mU/ml of BxTW1 expressed under standard conditions and in 50 mM formate buffer (pH 3) at 50°C for 10 min. The reaction was stopped by incubation at 100°C for 5 min. The presence and concentration of the remaining substrate and transxylosylation and hydrolysis products were determined by high-performance liquid chromatography (HPLC) on an Agilent 1200 series system equipped with a refractive index detector.

Aliquots of 100 μl were loaded onto a SUPELCOGEL C-G610H column (Sigma) equilibrated in 5 mM H_2SO_4 buffer. The column was previously calibrated by injecting 100 μl of xylose and XO samples, from X2 to X5, in a concentration range from 0.5 mM to 20 mM. From the area under the peaks, a calibration curve was calculated for each compound. Peaks were identified from their retention times, by comparison with those of the commercial standards, and their concentrations were calculated from the calibration curves. The results were used to estimate hydrolysis and transxylosylation ratios according to the equations below,

where the subscript zero indicates the initial concentration and the subscript *f* indicates the final concentration:

$$\frac{([\text{substrate}]_0 - [\text{substrate}]_f) - 2[\text{transxylosylation product}]_f}{[\text{substrate}]_0 - [\text{substrate}]_f} \times 100 = \text{hydrolysis ratio}$$

$$100 - \text{hydrolysis ratio} = \text{transxylosylation ratio}$$

In order to evaluate the acceptor specificity of the enzyme, 3.5 mM *p*NPX (as the xylose donor) was incubated for 240 min with 24 mU/ml of BxTW1, expressed under standard conditions, and 50 mM formate buffer (pH 3) in the presence of one of the following acceptors: 1 M methanol, ethanol, 1-propanol, 2-propanol, 1-butanol, isobutanol, or glycerol or 70 mg/ml erythritol, mannitol, sorbitol, dulcitol, glucose, fructose, galactose, mannose, maltose, sucrose, trehalose, or lactose. The selected acceptors were compared and grouped according to their physicochemical similarity after calculating the Tanimoto coefficient, using the workbench similarity tool from the ChemMine site (17). The reaction was stopped by incubation at 100°C for 5 min. The amount of free *p*NP released from substrate hydrolysis was measured spectrophotometrically, while the xylose content was determined by GC-MS, as described above. Transxylosylation, substrate hydrolysis, and substrate consumption ratios were calculated from the concentration of xylose and *p*NP according to the equations below:

$$\frac{[p\text{NPX}]_0 - [p\text{NP}]_{\text{free}}}{[p\text{NPX}]_0} \times 100 = \text{substrate consumption}$$

$$\frac{[p\text{NP}]_{\text{free}} - [\text{xylose}]_{\text{free}}}{[p\text{NP}]_{\text{free}}} \times 100 = \text{transxylosylation ratio}$$

$$100 - \text{transxylosylation ratio} = \text{hydrolysis ratio}$$

The results were presented as a heat map based on the transxylosylation ratios. The hierarchical clustering analysis was performed using the clustergram algorithm within the Matlab environment (MathWorks, Natick, MA).

The regioselectivity of BxTW1 when catalyzing the formation of a new glycosidic linkage was also investigated. In order to obtain one or more transxylosylation products, 350 mM xylobiose was incubated in 50 mM formate buffer (pH 3) at 50°C for 30 min with 550 mU/ml of BxTW1. In a second experiment, 3.5 mM *p*NPX used as the donor and 130 mM xylose used as the acceptor were incubated with 500 mU/ml of BxTW1 in 50 mM formate buffer (pH 3), at 50°C for 20 min, in order to obtain one or more transxylosylation products. Both reactions were stopped by heating at 100°C for 5 min. The samples were dried and resuspended in deuterated water. The identification of the transxylosylation products was accomplished by ^{1}H, ^{1}H-^{13}C HSQC (heteronuclear multiple-bond coherence), DOSY (diffusion-ordered spectroscopy), and DOSY-TOCSY (total correlation spectroscopy)-NMR on a Bruker 600 MHz spectrometer. The same approaches were applied to the commercial reagents added to each reaction, in order to discard signals from impurities and to confirm the assignations.

Peptide mass fingerprinting using MALDI-TOF mass spectrometry. Gel pieces of the BxTW1 protein bands from Sypro-stained SDS gels were excised and digested in accordance with a protocol based on a report by Shevchenko et al. (18) with minor variations as reported by Russo et al. (19). MALDI-MS and tandem MS (MS/MS) data were combined using the BioTools 3.0 program (Bruker-Daltonics) to interrogate the NCBI nonredundant (NCBInr) protein database using MASCOT software 2.3 (Matrix Science). Relevant search parameters were set as follows: trypsin as enzyme, carbamidomethylation of cysteines as fixed modification, methionine oxidation as variable modification, 1 missed cleavage allowed, peptide tolerance of 50 ppm, and MS/MS tolerance of 0.5 Da. Protein scores greater than 75 were considered significant ($P < 0.05$).

Primer design, amplification of BxTW1, and classification. To identify the gene coding for BxTW1, a BLASTP search against NCBInr using the peptides obtained by mass fingerprinting was carried out. The nucleotide sequences of the genes coding for β-xylosidases with high sequence identity to BxTW1 were retrieved from the database. Sequences were aligned using ClustalW, and degenerate primers were designed in the conserved 5′ and 3′ regions, including ATG and stop codons (BxTw1 Fw, 5′-ATGGTYTACACCRYGCAATWYCTG-3′, and BxTw1 Rv, 5′-TYAM YTRKRATCAGGYTKAATCTCC-3′). The BxTw1 gene was amplified by PCR using genomic DNA as the template. The DNA was extracted with the DNeasy Plant minikit (Qiagen), and PCR mixtures contained 100 ng of DNA template, 1× PCR buffer, 1.5 mM $MgCl_2$, 0.8 mM deoxynucleoside triphosphates (dNTPs), 0.5 μM each primer, and 1 U of *Taq* DNA polymerase (Invitrogen) in a final volume of 50 μl. Reaction mixtures were subjected to an initial denaturation at 94°C for 5 min; 34 cycles of amplification each at 94°C for 45 s, 55°C for 45 s, and 72°C for 2.5 min; followed by a final extension step at 72°C for 5 min. Control reactions lacking template DNA were simultaneously performed.

The amplified sequences were separated in a 0.8% (wt/vol) agarose electrophoresis gel stained with GelRed, cut out, and purified using a QIAquick gel extraction kit (Qiagen). PCR products were then inserted into a pGEM-T easy cloning system (Promega) in order to transform the *Escherichia coli* DH5α strain. Clones containing the inserted fragments were sequenced using the BigDye Terminator v3.1 cycle sequencing kit and the automated ABI Prism 3730 DNA sequencer. The coding sequence was used to carry out a BLASTN search against the NCBInr database in order to identify homologous proteins and include BxTW1 in the appropriate GH family.

Nucleotide sequence accession number. The nucleotide sequence for the BxTW1 gene was submitted to the GenBank database under accession number KP119719.

RESULTS

β-Xylosidase production. The secreted proteins and β-xylosidase activity of *T. amestolkiae* cultures were studied in Mandels medium with different carbon sources. Figure 1A shows the β-xylosidase inducer effect of 1% Avicel, 1% D-xylose, or 1%, 2%, or 3% beechwood xylan over 6 days. A control culture with 1% D-glucose as the carbon source, which inhibits xylanase production by carbon catabolite repression (20), was also tested. The highest β-xylosidase activity was detected when 2% beechwood xylan was used as the inductor, and the profile of total secreted proteins was similar to that detected with 3% xylan. Xylose addition also produced β-xylosidase release, although at a lower level. Figure 1B depicts the levels of secreted proteins over the culture time, with a sharp increase of extracellular proteins evident at the end of the period. At this point, a very fragmented mycelium was observed under the light microscope (data not shown), probably related to cellular lysis and the massive release of intracellular proteins. Based on these results, 2% beechwood xylan was chosen as the best inducer for β-xylosidase, which was purified and characterized from these crude proteins. For additional data on the high abundance of BxTW1 in the secretome of *T. amestolkiae* under the conditions selected here, see Fig. S1 and the "secretome" section in the supplemental material.

Purification of β-xylosidase. Maximal β-xylosidase activity levels (800 mU/ml) were detected in 3-day-old cultures. Then, these crude proteins were collected for enzyme purification. The first cation-exchange chromatography step allowed the separation of a unique peak with β-xylosidase activity, eluting around 0.25 M NaCl, from most of the crude proteins. The peak with β-xylosidase activity was subsequently separated on a Mono S 5/50 high-resolution cation-exchange column. β-Xylosidase activity mainly eluted in three successive peaks between 0.20 and 0.25 M NaCl. A last step using a high-resolution Superose 12 column was neces-

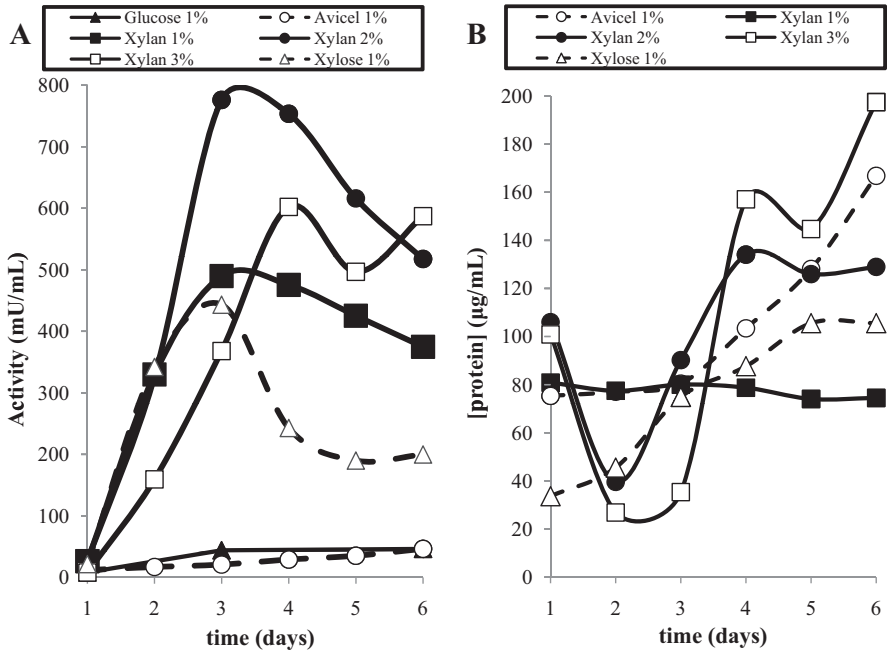

FIG 1 Extracellular β-xylosidase activity (A) and protein concentration (B) of *T. amestolkiae* cultures in Mandels medium in the presence of different carbon sources.

sary for the complete purification of the protein, which was named BxTW1. The enzyme, dialyzed and concentrated, was stored at 4°C, remaining stable over at least 6 months. The purification resulted in a final yield of 10.8% recovered activity. During the process, the specific activity increased from 1.0 to 47.1 U/mg, which implies a degree of purification of 47.

Physicochemical properties. The molecular mass of BxTW1, estimated from size-exclusion chromatography, was around 200 kDa. However, analysis of the BxTW1 gene sequence (GenBank accession no. KP119719) using the ExPASY Bioinformatics Resource Portal resulted in a theoretical molecular mass of 84,373.96 Da. SDS-PAGE of nondeglycosylated BxTW1 showed three bands of approximately 100 kDa (Fig. 2A), which is close to the value from MALDI-TOF MS (Fig. 2B). The MALDI-TOF spectrum displayed the typical profile of a glycosylated protein, with a wide peak due to glycosylation heterogeneity. The technique allowed determination of the accurate mass of one of the glycosylated isoforms (102,275 kDa), but the global enzyme mass could only be estimated on average ca. 100 kDa. The closeness of the peaks in the mass spectrum apparently corresponded to three different glycosylation forms, which would be consistent with the identification of three separated peaks of β-xylosidase activity during high-resolution cation-exchange chromatography. The peptide mass fingerprint of each one of the three bands was obtained, resulting in exactly the same fragmentation patterns (not shown). To discern if these molecular mass changes could be due to glycosidic content

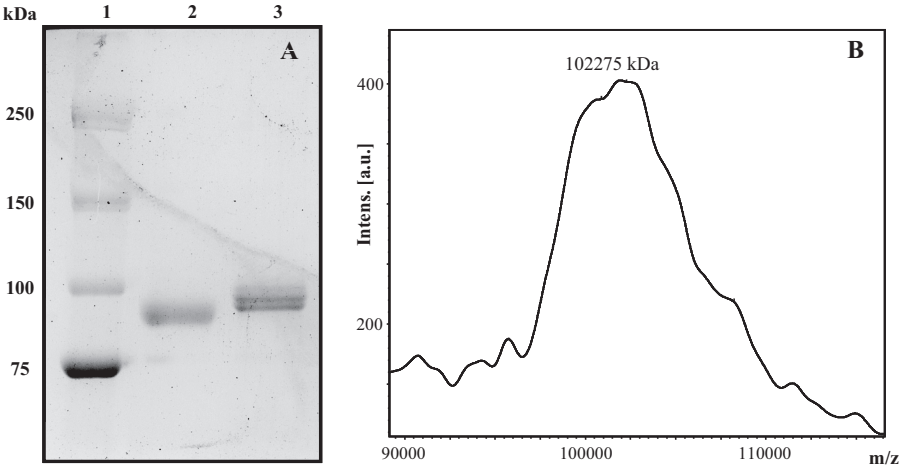

FIG 2 Estimation of BxTW1 molecular mass by SDS-PAGE (A) and MALDI-TOF MS (B). Lanes: 1, molecular mass standards; 2, BxTW1 treated with Endo H; 3, glycosylated BxTW1. Intens., intensity; a.u., arbitrary units.

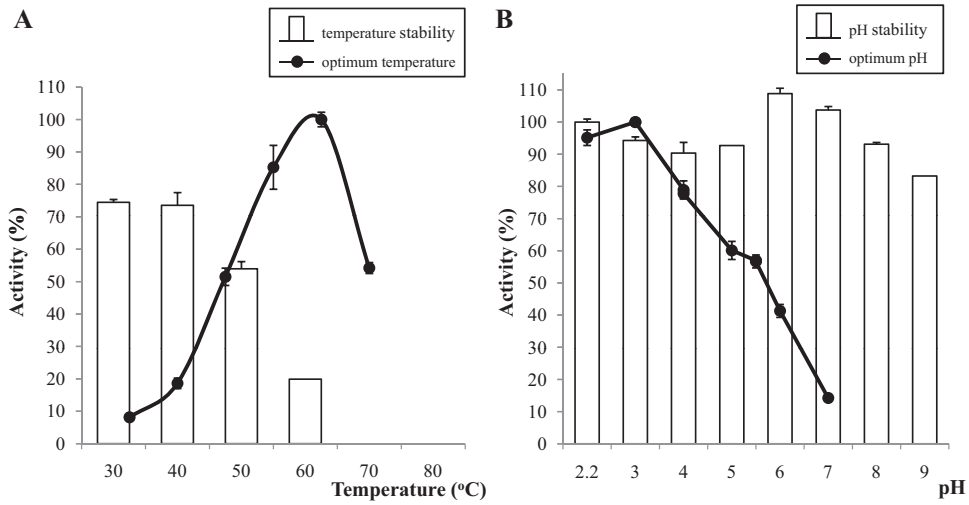

FIG 3 Effect of temperature (A) and pH (B) on BxTW1 activity. (A) The line indicates the effect of temperature on enzyme activity, and the bars show its stability in a range of temperatures from 30°C to 70°C after 72 h. (B) The line corresponds to the effect of pH on enzyme activity, and the bars show its stability in a range of pH from 2.2 to 9 after 72 h.

variations, the mature protein sequence was used to search for predicted posttranslation modifications on the ELM server, and 14 motifs for N-glycosylation were found. In addition, after Endo H treatment, only one band was detected, with a molecular mass close to the theoretical value of 84 kDa, corroborating the existence of three different glycosylation isoforms of BxTW1 instead of three different isoenzymes. The difference between the molecular masses determined by size-exclusion chromatography and SDS-PAGE suggests that BxTW1 works as a noncovalent dimer in its native conformation.

Isoelectrofocusing indicated that the pI of the protein was 7.6, a value similar to those reported for other β-xylosidases (20). Nevertheless, the theoretical value obtained from the BxTW1 sequence was 4.75. This difference was not surprising, since it has been extensively reported that glycosylation can change the isoelectric point of a protein (21).

The influence of temperature and pH on stability and optimal reaction activity of BxTW1 was tested against *p*NPX. The optimum temperature (highest hydrolysis rate) was 70°C, although the enzyme lost 70% activity after 30 min at 60°C (data not shown). At 50°C, the activity loss stabilized around 50% after 1 h (data not shown) and remained stable for 72 h (Fig. 3A). The thermal index T50 was 59.9°C. Regarding pH, BxTW1 displayed its maximal activity at pH 3 and exhibited high stability (above 80% of residual activity) between pH 2.2 and 9 for 72 h (Fig. 3B).

BxTW1 activity did not show relevant changes in the presence of most of the tested compounds when sodium acetate or citrate buffers at pH 5 were used (Fig. 4). When small inhibition rates were observed, the residual activities were slightly higher in the presence of citrate, probably due to its chelating properties. The most remarkable results were the slight inhibition registered during the addition of Cu^{2+} and Pb^{2+} in both buffers and the dramatic decrease of activity in the presence of Hg^{2+}. The absence of inhibition in the presence of EDTA, DTT, and 2-mercaptoethanol suggest that BxTW1 does not require metallic cations for its catalytic activity and the absence of a disulfide bond near or inside the active site. The nondependence of metal cofactors is a common feature of GH3 proteins, but there are a few solved structures displaying disulfide bonds within this group (22, 23).

Substrate specificity. The enzyme hydrolyzed *p*NPX, *p*NP-α-L-arabinopyranoside, *p*NP-α-L-arabinofuranoside, and xylooligosaccharides (XOs) from X2 to X6 and was capable of releasing xylose from beechwood xylan. Nevertheless, no activity was detected on other nitrophenyl substrates or disaccharides assayed. The kinetic parameters of BxTW1 (Table 1) were determined using the specific substrates reported above. Although the enzyme was able to hydrolyze *p*NP-α-L-arabinoside independently of the glycan moiety configuration, its affinity toward these substrates was much lower than that found for *p*NPX. The hydrolytic mechanism of BxTW1 was ascertained by ^{1}H-NMR, with xylose release analyzed during the first minutes of the reaction. Like all the GH3 family members, BxTW1 worked with a retaining mechanism (for the NMR data, see the "analysis of the hydrolytic mechanism of BxTW1" section in the supplemental material). The enzyme also hydrolyzed XOs of different chain lengths with similar affinities, from 3 to 6 xylose units, but with decreasing catalytic efficiency. Surprisingly, the enzyme attacked X3 to X6 with higher affinity than X2. Since K_m values were calculated by estimating the released xylose instead of monitoring substrate consumption, and in order to confirm that BxTW1 hydrolyzed X3 preferentially over X2, xylotriose consumption and xylobiose generation were monitored by ^{1}H-NMR spectroscopy (Fig. 5A). Comparison of spectra revealed the preference of BxTW1 for the trisaccharide over the released disaccharide (Fig. 5B). This result unequivocally demonstrated xylotriose consumption and agreed with global K_m values for XOs calculated from the xylose released. Enzyme inhibition by product was also studied, revealing that the activity against *p*NPX was competitively inhibited by xylose, with a K_i of 1.7 mM.

Transxylosylation. The transxylosylation capabilities of BxTW1 were tested. Xylotriose and xylobiose were first assayed as simultaneous donors and acceptors in separate reactions. This double role of substrates has been previously reported (24). Since the enzyme preferentially hydrolyzes X3 over X2 (Fig. 5), differences in transxylosylation rates were also analyzed as a function of the

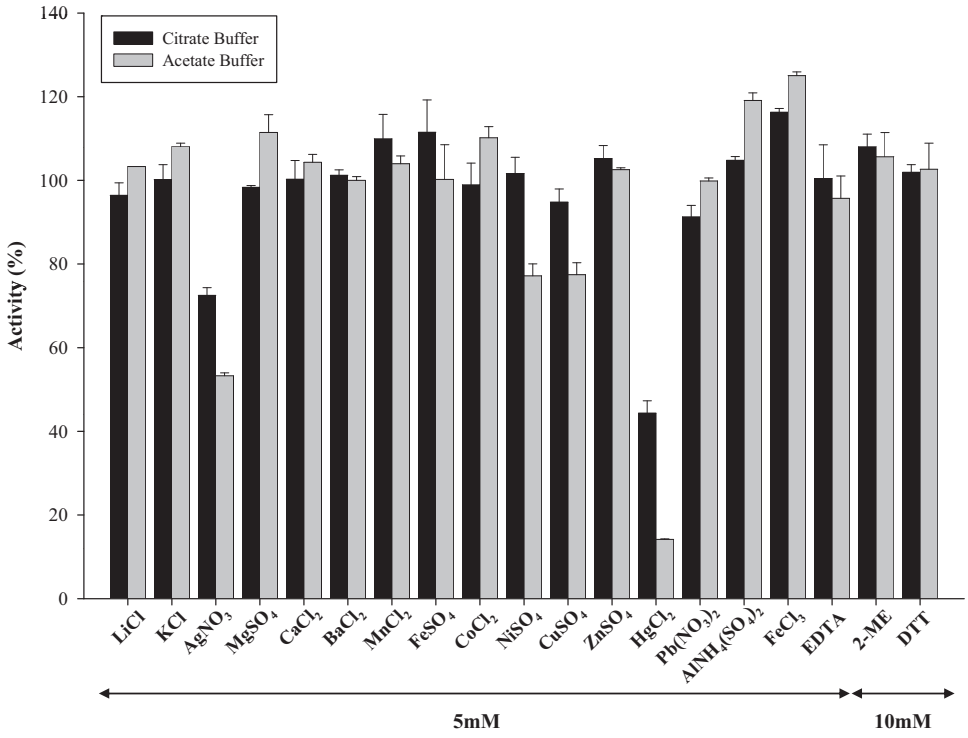

FIG 4 Effects of some chemical compounds on BxTW1 activity.

acceptor length and concentration. In this work, a direct relation between acceptor concentration and the synthesis of transxylosylation products was observed (Fig. 6). On the other hand, xylotriose was synthetized from xylobiose, and when xylotriose was used as the substrate, the resultant product was xylotetraose. In both cases, transxylosylation ratios increased with the substrate concentrations (detection limit, above 5 mM substrate). Below 10 mM, transxylosylation rates were comparable using X2 or X3. However, X2 was a better transxylosylation acceptor than X3 at concentrations over 20 mM (ca. 40% transxylosylation rate versus 30%, respectively). Figure 6 shows the evolution of transxylosylation and hydrolysis ratios using xylobiose (Fig. 6A) and xylotriose (Fig. 6B) as substrates.

The transxylosylation specificity of BxTW1 was tested in reactions with *p*NPX as the donor and a large excess of different acceptors, measuring xylose/*p*NP ratios at the final reaction time. To calculate transxylosylation rates, the stoichiometric relation between products (xylose and *p*NP) was taken as 1:1. Then, detection of *p*NP at a significantly higher concentration than xylose for an assayed acceptor indicates that transxylosylation occurred and the monosaccharide has been attached to the acceptor. A variety of alkyl alcohols, sugar alcohols, monosaccharides, and disaccharides were tested as acceptors. A low transxylosylation rate of 13% was observed in the absence of an acceptor, showing that BxTW1 was capable of using *p*NPX molecules as acceptors. The consumed substrate exceeded 80% in all cases, and the highest transxylosylation rates were obtained mainly with alkan-1-ols, alkan-2-ols, and sugar alcohols (Fig. 7A), while monosaccharides and disaccharides turned out to be the worst acceptors. Chemical similarities between acceptors were estimated by a Tanimoto coefficient calculation, and a comparative analysis was carried out using the hierarchical clustering tool from the MatLab environment (Fig. 7B). The results showed that compounds with very close physicochemical features behave differently as transxylosylation acceptors. Regarding sugar alcohols, mannitol is a much better acceptor than sorbitol and dulcitol, although all of them have the same

TABLE 1 Kinetic parameters of BxTW1 against different substrates

Substrate	K_m (mM) (mean ± SD)	V_{max} (U/mg) (mean ± SD)	k_{cat} (s^{-1})	k_{cat}/K_m ($mM^{-1} \cdot s^{-1}$)
*p*NPX	0.17 ± 0.01	52.0 ± 0.5	173	1,000
*p*NP-α-L-arabinopyranoside	3.6 ± 0.3	66.9 ± 4.2	220	62
*p*NP-α-L-arabinofuranoside	5.8 ± 0.4	43.0 ± 1.7	143	25
Xylobiose	0.48 ± 0.05	55.2 ± 1.3	183	380
Xylotriose	0.22 ± 0.01	19.8 ± 0.3	66.1	290
Xylotetraose	0.20 ± 0.01	15.4 ± 0.1	51.2	260
Xylopentaose	0.20 ± 0.01	11.8 ± 0.2	39.2	200
Xylohexaose	0.22 ± 0.01	9.5 ± 0.1	32	140
Xylan	7.0 ± 0.2[a]	68.7 ± 0.6	229	

[a] The K_m value for xylan is in milligrams per milliliter.

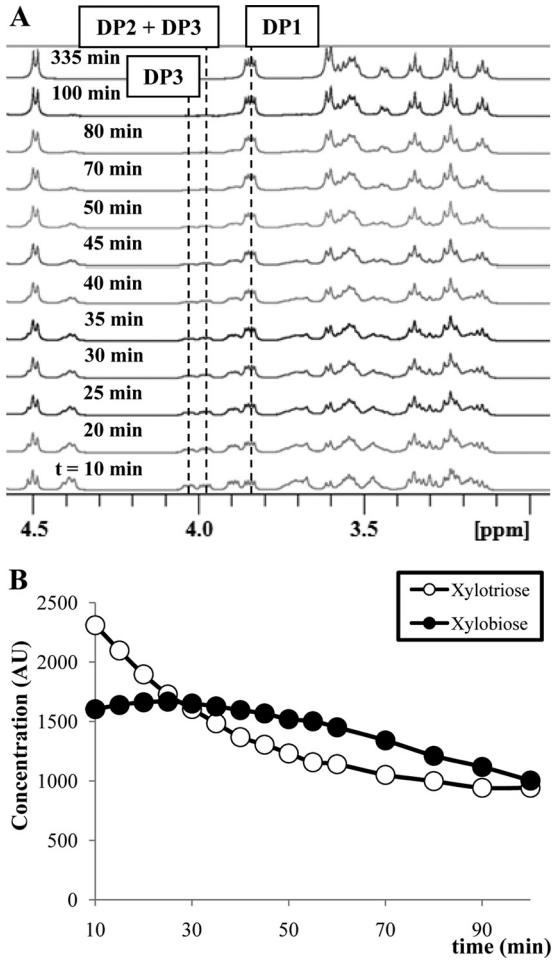

FIG 5 (A) Proton NMR spectra of xylotriose consumption by BxTW1 over time. Signals using for quantification are indicated by vertical dashed lines. (B) Evolution of xylotriose and xylobiose concentration during the reaction time. Concentrations were determined by integrating the appropriate signals of each compound.

molecular formula. In the case of aldoses, glucose, galactose, and mannose also share the same empirical formula but were very different as acceptors: glucose was the most efficient, while transxylosylation yields for galactose were significantly lower.

The regioselectivity of BxTW1 when catalyzing the formation of a new glycosidic linkage, using xylobiose or xylose as the acceptor, was also investigated. Xylobiose was used as a simultaneous donor and acceptor for the synthesis of either the trisaccharide or higher-DP transxylosylation products. A DOSY-NMR spectrum of the reaction mixture was acquired, and the detected signals could be correlated with the presence of mono-, di-, and trisaccharides. DOSY-TOCSY and ^{1}H-^{13}C HSQC-NMR spectra were acquired in order to simplify the assignation of ^{1}H one-dimensional NMR (1D-NMR) signals. The chemical shift displacement data allowed us to conclude that BxTW1 catalyzed the regioselective synthesis of 1,4-β-D-xylotriose as a unique transxylosylation product. BxTW1 regioselectivity was also tested using *p*NPX as the donor and xylose as the acceptor, to test if the reaction products were disaccharides or had higher DPs. A ^{1}H-NMR spectrum was acquired from the reaction mixture, and ^{1}H-^{13}C HSQC-NMR data were used to simplify the analysis. The assignation of signals indicated that BxTW1 catalyzed the synthesis of 1,4-β-D-xylobiose as the unique transxylosylation product.

Sequencing, classification, and molecular characterization of BxTW1. The preliminary identification of BxTW1 was based on its peptide mass fingerprint. The three bands identified in SDS-PAGE gels as glycosylated isoforms of BxTW1 were analyzed, giving the same profile of tryptic peptides. The homology search of these peptides revealed close similarities of the BxTW1 enzyme to four putative fungal β-xylosidases from *Talaromyces stipitatus* ATCC 10500 (GI:242771939), *Talaromyces cellulolyticus* (GI:348604625), *Talaromyces marneffei* ATCC 18224 (GI:212531051), and *Hypocrea orientalis* strain EU7-22 (GI:380293099) and three β-xylosidases isolated from *Trichoderma reesei* (GI:2791277), *Talaromyces emersonii* (GI:48526507), and *Aspergillus fumigatus* (GI:76160897).

Gene sequencing revealed that a 2,394-bp region with no introns codes for BxTW1 (GenBank accession number KP119719). A homology search based on DNA sequence showed high identity

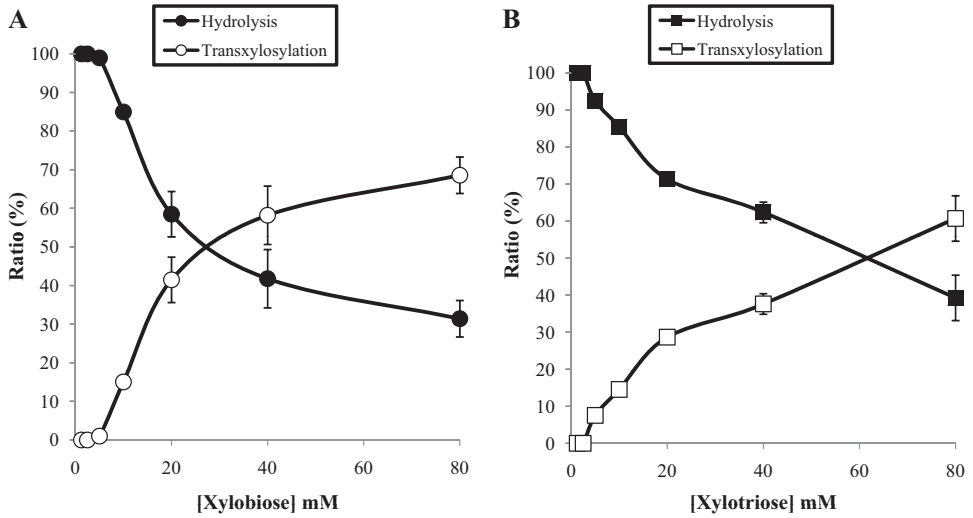

FIG 6 Transxylosylation ratios according to the initial substrate concentration. Reaction products and substrate were separated by HPLC. Ratios were obtained by comparing areas under the curves of the remaining substrate and the product of transxylosylation.

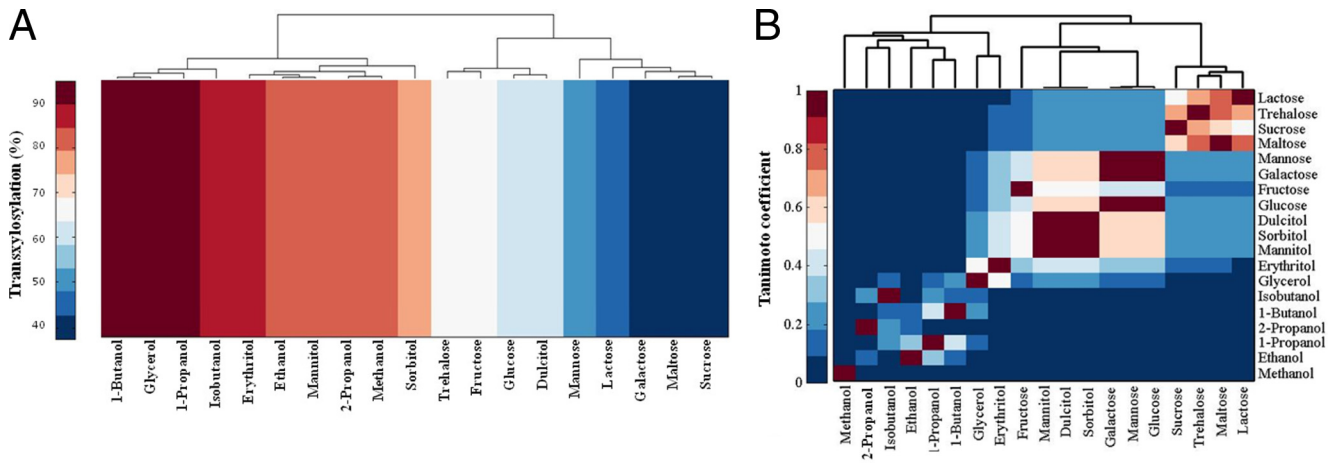

FIG 7 (A) Transxylosylation ratios of BxTW1 in the presence of different acceptors. Acceptor specificity is presented as a heat map based on transxylosylation ratios. The hierarchical clustering analysis was performed using the clustergram algorithm within the Matlab environment (MathWorks, Natick, MA). (B) Hierarchical clustering of the chemical similarity of the acceptors as estimated by Tanimoto coefficient calculation using the ChemMine program. Clustering was performed within the Matlab environment.

of BxTW1 with putative β-xylosidases from *T. stipitatus* ATCC 10500 (GI:242771939), *T. cellulolyticus* (GI:348604625), and *T. marneffei* ATCC 18224 (GI:212531051), all of them belonging to the GH3 family and with their corresponding genes lacking introns.

These data indicate that BxTW1 from *T. amestolkiae* is a β-xylosidase from the GH3 family. For the phylogenetic validation of this classification, see Fig. S2 and the "identification of BxTW1 GH family" section in the supplemental material.

DISCUSSION

The identification and characterization of β-xylosidases are currently noteworthy topics. The need for biomass exploitation in order to obtain goods from renewable sources and the synthesis of xylooligosaccharides by transxylosylation makes these enzymes very interesting from a biotechnological perspective.

In this context, the β-xylosidase levels released by *T. amestolkiae* in liquid cultures are in agreement with previous results described for *Aspergillus* and *Fusarium* strains when beechwood xylan was added as a carbon source (25, 26) and higher than those reported for other *Penicillium* species (27, 28). Although pure commercial xylan is not suitable for large-scale enzyme production, it has been established as the most used carbon source and the best inducer of xylanolytic enzymes (29). As in other fungi, xylose acts as a weak inducer of β-xylosidase production in *T. amestolkiae* (30), but glucose did not induce β-xylosidase production (30, 31).

The study of the effect of temperature, pH, and common chemicals on BxTW1 activity revealed some remarkable properties. The optimum pH value of 3.0 was surprising, since most of the described fungal β-xylosidases displayed values from 4.0 to 6.0 (20), and few enzymes with this optimum value (32) or lower (33) have been described. The causes for this low pH value remain unknown. Sequence alignments of BxTW1 and closely related GH3 xylosidases (data not shown) revealed no changes in the catalytic environment that would explain the low optimum pH of BxTW1. However, Rasmussen et al. (34) reported that β-xylosidases from *T. emersonii* and *T. reesei* changed their optimum pH from pH 4.0 to pH 3.0 to 3.5 when they were expressed in *Aspergillus oryzae*, for which high N-glycosylation potential has been reported (35). This observation could suggest that this posttranslational modification might modulate the pH sensitivity of glycoside hydrolases. N-oligosaccharides may display charged substituents (36) which could affect pH sensitivity by changing the pI or modifying the pK_a value of close amino acids. In the case of BxTW1, N-glycosylation has been determined by SDS-PAGE after Endo H treatment and by *in silico* analysis, with the conclusion that the reported difference between theoretical and experimental pI values could be explained by these modifications. According to these findings, the low optimum pH of BxTW1 could also be related to its glycosylation pattern and not to differences in the amino acid sequence of the active site. The broad stability pattern of the *T. amestolkiae* enzyme was also notable, covering acidic and basic values, while most of the characterized fungal β-xylosidases are quickly inactivated at extreme (low or high) pH values (26, 37). Both stability and high activity at low pH values make it a good candidate to be used in 2G bioethanol production or as supplements for animal feed.

The absence of BxTW1 inhibition in the presence of several heavy metals that commonly inactivate β-xylosidases merits especial attention. The resistance is particularly important in the case of Cu^{2+}, which has been reported as a strong inhibitor of many β-xylosidases (38, 39) and present in the ash content of different lignocellulosic biomasses, showing inhibitory effects on cellulases and reducing the final yield of 2G bioethanol production even at low concentrations (40).

Regarding its kinetic characterization, although the maximum velocity of BxTW1 was comparable to those reported for other fungal β-xylosidases (Table 2), the results showed a remarkable high affinity of the enzyme to *p*NPX. Very few characterized β-xylosidases, such as BXTE from *T. emersonii* (34), had a slightly lower K_m value toward this substrate. Nevertheless, BxTW1 demonstrated better kinetic properties: its V_{max} is 22-fold higher than that of Xyl I, and the k_{cat} against *p*NPX was 173 s^{-1}, more than 700-fold higher than that reported for BXTE. Catalytic efficiency, an extensively used parameter for enzyme comparison (41), is also

TABLE 2 Comparative kinetic parameters for different fungal β-xylosidases using *p*NPX as the model substrate

Organism	Enzyme[b]	K_m (mM)	V_{max} (U/mg)	k_{cat} (s^{-1})	k_{cat}/K_m ($mM^{-1} \times s^{-1}$)	Reference
Talaromyces amestolkiae	BxTW1	0.17	52.0	173	1,000	This work
Aspergillus awamori	X-100	0.25		17.5	70	49
Aspergillus carbonarius		0.20	3.64			50
Aspergillus japonicus		0.31	114	215[a]	690[a]	51
Aspergillus nidulans		1.1	25.6	76.8[a]	70[a]	52
Aspergillus ochraceus		0.66	39			53
Aureobasidium sp.	Bxyl	2	940	5,500	2,750	54
Fusarium proliferatum		0.77	75			39
Fusarium verticilloides		0.85				26
Humicola grisea	Bxyl	0.48				49
	Bxyl	1.37	13.0	1.22×10^{-5}	1×10^{-5}	49
Humicola insolens		1.74	22.2		3,900	49
Penicillium sclerotium		0.78	0.51	1.2[a]	1.6[a]	28
Scytalidium thermophilum	Bxyl	1.7	88	66[a]	38.8[a]	55
Sporotrichum thermophile	Intracell Bxyl	1.1	114	89.3[a]	81[a]	56
Talaromyces emersonii	BXTE	0.06		0.017	0.3[a]	34
	Xyl I	0.13	1.7	430	3,300	49
	Xyl II	32.9	6.3	900	27	49
	Xyl III	1.4	0.26	61	44	49
Talaromyces thermophilus	Bxyl	2.37	0.049	0.037[a]	0.016[a]	57
Trichoderma reesei	BXTR	0.8		0.015	0.02	49
Trichoderma viride		5.8		21.3	3.7	58

[a] Not included in the original article but calculated with data provided.
[b] Where no enzyme name is provided, the enzyme described did not have a name listed in the original article.

shown for each enzyme, when available, in Table 2. The efficiency of BxTW1 is among the highest values reported. In fact, β-xylosidase from *Bacillus pumilus*, commercialized by Megazyme (SKU code E-BXSEBP), shows a catalytic efficiency of 230 $mM^{-1} \cdot s^{-1}$, calculated from the reported data (42), a value 4.5-fold lower than that of BxTW1.

Although the activity of the enzyme toward xylobiose is in the range of the highest values found in literature (43), it showed higher affinity toward longer substrates (X3 to X6). Even though kinetic characterization of β-xylosidases against XOS with a DP higher than xylobiose has not been extensively studied, a detailed comparison revealed that BxTW1 had the highest catalytic efficiency for all the XOs tested from X3 to X6. In fact, the kinetic constants of BxTW1were frequently 1 or 2 orders of magnitude greater than those of characterized β-xylosidases (Table 3). In addition, BxTW1 showed activity against beechwood xylan, something uncommon among most of the known β-xylosidases. These behaviors have been previously reported, and they are considered a typical feature of exo-type xylanolytic enzymes (34, 44), in contrast to classical β-xylosidases (45). Exo-type xylanases (EC 3.2.1.156) are also called reducing-end xylose-releasing exo-oligoxylanases (Rex enzymes), and they share with β-xylosidases (EC 3.2.1.37) the exo-attack of substrates. Nevertheless, there are several differences suggesting that BxTW1 should be identified as a

TABLE 3 Comparison of catalytic efficiencies against XOS from X2 to X3 of fungal and bacterial β-xylosidases

		k_{cat}/K_m ($mM^{-1} \cdot s^{-1}$)					
Organism	Enzyme	X2	X3	X4	X5	X6	Reference
Talaromyces amestolkiae	BxTW1	382	287	258	198	143	This work
Aspergillus nidulans	BxlA	70	58	42	33	22	47
	BxlB	14	9	8	5	4	47
Alkaliphilus metalliredigens	AmX	39.4	30.7				59
Bacillus pumilus	BpX	7.45	6.10	1.42			59
Bacillus subtilis	BsX	56.6	35.2	1.42			59
Geobacillus thermoleovorans	GbtXyl43A	5.1×10^{-3}	3.9×10^{-3}				60
Lactobacillus brevis	LbX	138	80.8	2.40			59
Aspergillus oryzae[a]	XylA	13.8	9.7	33.1			61
Neurospora crassa[a]		3.4	1.4	0.7			62
Selenomonas ruminantium	SXA	90.2	44.8	33.3	27.0	26.1	63

[a] Recombinant protein expressed in *P. pastoris*.

β-xylosidase. As mentioned above, alignment studies revealed high homology between BxTW1 and other putative and characterized β-xylosidases. In addition, all the reported Rex enzymes are included in the GH8 family, work with inversion of the configuration, and are unable to hydrolyze xylobiose (46). These data strongly suggest that BxTW1 cannot be considered a Rex enzyme and should be considered a β-xylosidase.

BxTW1 demonstrated transxylosylation capacity, and rates increased with substrate concentration when xylobiose and xylotriose were used as the donor and acceptor simultaneously. The transxylosylation and hydrolytic rates were complementary, since the longest substrate was a worse acceptor than the shortest.

BxTW1 showed broad acceptor specificity. Short alkan-ols were the best acceptors, probably due to their low molecular mass and to the physicochemical properties of the enzyme's active site, such as its size or hydrophobicity. The results suggested that aldoses and alcohols were preferentially transxylosylated on primary alcohols, since 1-propanol and 1-butanol were better acceptors than 2-propanol and isobutanol, respectively. To confirm this, aldohexoses distinguished only by their three-dimensional spatial orientation were used as acceptors. In D-glucose, all hydroxyl groups but the primary one (C-6) are in equatorial position and, hence, the transxylosylation rates were higher than those obtained with D-mannose, where the C-2 hydroxyl group shares the axial position with the primary alcohol. The transxylosylation rate was even lower when D-galactose was used as the acceptor, where the axial position was occupied by a C-4 hydroxyl (closer than C-2 to the primary alcohol). No clear conclusions could be drawn from the results obtained when sugar alcohols or disaccharides were used as acceptors; in these cases, unknown steric hindrances may occur. A deeper understanding of the residues and mechanism involved in transxylosylation reactions would be necessary to decipher acceptor specificity (24, 47). Currently, a complete structural analysis of BxTW1 is being carried out in order to grasp its hydrolytic and transxylosylation capacities.

Both its promiscuity and its efficiency suggest a considerable potential of BxTW1 for the biosynthesis of oligosaccharides with pharmacological or industrial interest. The enzymatic synthesis of new oligosaccharides by transglycosylation is a promising alternative to chemical methods. Many glycosidases have been studied in order to determine their ability to form a glycosidic bond stereospecifically, but most of them show low regioselectivity. This implies that the transglycosylation products are multiple instead of unique, hence hampering their use for industrial production. Few glycosidases with regioselectivity have been described previously, which has been related to their specificity (48). In this sense, although the regioselectivity of BxTW1 has been analyzed only when xylose or xylobiose was used as the acceptor, its broad substrate specificity makes it a good candidate to test different and new molecules as final xylose receivers. This reinforces the potential of BxTW1 for the biosynthesis of new oligosaccharides with potential industrial interest.

ACKNOWLEDGMENTS

This work was carried out with funding from the MINECO projects PRIPIBAR-2011-1402 and RTC-2014-1777-3 and the Comunidad de Madrid Program RETO-PROSOT S2013/MAE-2907. M. Nieto-Domínguez thanks the MINECO for an FPU fellowship.

We thank F. J. Cañada and J. Jiménez-Barbero for their help in the development of NMR experiments and J. Nogales for his help in the development of hierarchical clustering analysis. We are grateful for the use the Gas Chromatography and Proteomics and Genomic facilities at CIB.

REFERENCES

1. **Naik S, Goud VV, Rout PK, Dalai AK.** 2010. Production of first and second generation biofuels: a comprehensive review. Renew Sustain Energy Rev **14:**578–597. http://dx.doi.org/10.1016/j.rser.2009.10.003.
2. **Zhang X, Zhu Y, Zhang Y, Liu Y, Liu S, Guo J, Li R, Wu S, Chen B.** 2014. Growth and metal uptake of energy sugarcane (*Saccharum* spp.) in different metal mine tailings with soil amendments. J Environ Sci (China) **26:**1080–1089. http://dx.doi.org/10.1016/S1001-0742(13)60543-4.
3. **Xie J, Weng Q, Ye GY, Luo SS, Zhu R, Zhang AP, Chen XY, Lin CX.** 2014. Bioethanol production from sugarcane grown in heavy metal-contaminated soils. Bioresources **9:**2509–2520.
4. **Talebnia F, Karakashev D, Angelidaki I.** 2010. Production of bioethanol from wheat straw: an overview on pretreatment, hydrolysis and fermentation. Bioresour Technol **101:**4744–4753. http://dx.doi.org/10.1016/j.biortech.2009.11.080.
5. **Kuhad RC, Gupta R, Khasa YP, Singh A, Zhang Y.** 2011. Bioethanol production from pentose sugars: current status and future prospects. Renew Sustain Energy Rev **15:**4950–4962. http://dx.doi.org/10.1016/j.rser.2011.07.058.
6. **Bao L, Huang Q, Chang L, Sun Q, Zhou J, Lu H.** 2012. Cloning and characterization of two beta-glucosidase/xylosidase enzymes from yak rumen metagenome. Appl Biochem Biotechnol **166:**72–86. http://dx.doi.org/10.1007/s12010-011-9405-x.
7. **Pastor F, Gallardo O, Sanz-Aparicio J, Drouet P.** 2007. Xylanases: molecular properties and applications, p 65–82. *In* Polaina J, McCabe AP (ed), Industrial enzymes: structure, function and applications. Springer, Dordrecht, The Netherlands.
8. **Rye CS, Withers SG.** 2000. Glycosidase mechanisms. Curr Opin Chem Biol **4:**573–580. http://dx.doi.org/10.1016/S1367-5931(00)00135-6.
9. **Azevedo Carvalho AF, Oliva Neto P, Da Silva DF, Pastore GM.** 2013. Xylo-oligosaccharides from lignocellulosic materials: chemical structure, health benefits and production by chemical and enzymatic hydrolysis. Food Res Int **51:**75–85. http://dx.doi.org/10.1016/j.foodres.2012.11.021.
10. **Torres P, Poveda A, Jimenez-Barbero J, Parra JL, Comelles F, Ballesteros AO, Plou FJ.** 2011. Enzymatic synthesis of alpha-glucosides of resveratrol with surfactant activity. Advanced Synthesis & Catalysis **353:**1077–1086. http://dx.doi.org/10.1002/adsc.201000968.
11. **Chavez R, Bull P, Eyzaguirre J.** 2006. The xylanolytic enzyme system from the genus *Penicillium*. J Biotechnol **123:**413–433. http://dx.doi.org/10.1016/j.jbiotec.2005.12.036.
12. **Gil-Muñoz J.** 2015. Estudio de las β-glucosidasas del complejo celulolítico de *Talaromyces amestolkiae*: caracterización y aplicaciones biotecnológicas. PhD thesis, Universidad Complutense, Madrid, Spain.
13. **Freixo MR, de Pinho MN.** 2002. Enzymatic hydrolysis of beechwood xylan in a membrane reactor. Desalination **149:**237–242. http://dx.doi.org/10.1016/S0011-9164(02)00769-5.
14. **Notararigo S, Nácher-Vázquez M, Ibarburu I, Werning ML, de Palencia PF, Dueñas MT, Aznar R, López P, Prieto A.** 2013. Comparative analysis of production and purification of homo- and hetero-polysaccharides produced by lactic acid bacteria. Carbohydr Polym **93:**57–64. http://dx.doi.org/10.1016/j.carbpol.2012.05.016.
15. **Yan Q, Wang L, Jiang Z, Yang S, Zhu H, Li L.** 2008. A xylose-tolerant beta-xylosidase from *Paecilomyces thermophila*: characterization and its co-action with the endogenous xylanase. Bioresour Technol **99:**5402–5410. http://dx.doi.org/10.1016/j.biortech.2007.11.033.
16. **Wasay SA, Barrington SF, Tokunaga S.** 1998. Remediation of soils polluted by heavy metals using salts of organic acids and chelating agents. Environ Technol **19:**369–379. http://dx.doi.org/10.1080/09593331908616692.
17. **Backman TW, Cao Y, Girke T.** 2011. ChemMine tools: an online service for analyzing and clustering small molecules. Nucleic Acids Res **39:**W486–W491. http://dx.doi.org/10.1093/nar/gkr320.
18. **Shevchenko A, Tomas H, Havlis J, Olsen JV, Mann M.** 2006. In-gel digestion for mass spectrometric characterization of proteins and proteomes. Nat Protoc **1:**2856–2860.

19. **Russo P, de la Luz Mohedano M, Capozzi V, Fernandez de Palencia P, Lopez P, Spano G, Fiocco D.** 2012. Comparative proteomic analysis of *Lactobacillus plantarum* WCFS1 and ΔctsR mutant strains under physiological and heat stress conditions. Int J Mol Sci **13:**10680–10696. http://dx.doi.org/10.3390/ijms130910680.
20. **Knob A, Terrasan C, Carmona E.** 2010. β-Xylosidases from filamentous fungi: an overview. World J Microbiol Biotechnol **26:**389–407. http://dx.doi.org/10.1007/s11274-009-0190-4.
21. **Marsh JW, Denis J, Wriston JC.** 1977. Glycosylation of *Escherichia coli* L-asparaginase. J Biol Chem **252:**7678–7684.
22. **Varghese JN, Hrmova M, Fincher GB.** 1999. Three-dimensional structure of a barley beta-D-glucan exohydrolase, a family 3 glycosyl hydrolase. Structure **7:**179–190. http://dx.doi.org/10.1016/S0969-2126(99)80024-0.
23. **Suzuki K, Sumitani JI, Nam YW, Nishimaki T, Tani S, Wakagi T, Kawaguchi T, Fushinobu S.** 2013. Crystal structures of glycoside hydrolase family 3 beta-glucosidase 1 from *Aspergillus aculeatus*. Biochem J **452:**211–221. http://dx.doi.org/10.1042/BJ20130054.
24. **Kurakake M, Fujii T, Yata M, Okazaki T, Komaki T.** 2005. Characteristics of transxylosylation by beta-xylosidase from *Aspergillus awamori* K4. Biochim Biophys Acta **1726:**272–279. http://dx.doi.org/10.1016/j.bbagen.2005.08.009.
25. **Lenartovicz V, de Souza CGM, Moreira FG, Peralta RM.** 2003. Temperature and carbon source affect the production and secretion of a thermostable β-xylosidase by *Aspergillus fumigatus*. Process Biochem **38:**1775–1780. http://dx.doi.org/10.1016/S0032-9592(02)00261-3.
26. **Saha BC.** 2001. Purification and characterization of an extracellular beta-xylosidase from a newly isolated *Fusarium verticillioides*. J Ind Microbiol Biotechnol **27:**241–245. http://dx.doi.org/10.1038/sj.jim.7000184.
27. **Jørgensen H, Mørkeberg A, Krogh KBR, Olsson L.** 2005. Production of cellulases and hemicellulases by three *Penicillium* species: effect of substrate and evaluation of cellulase adsorption by capillary electrophoresis. Enzyme Microb Technol **36:**42–48. http://dx.doi.org/10.1016/j.enzmictec.2004.03.023.
28. **Knob A, Carmona EC.** 2011. Purification and properties of an acid beta-xylosidase from *Penicillium sclerotiorum*. Ann Microbiol **62:**501–508.
29. **Milagres AMF, Lacis LS, Prade RA.** 1993. Characterization of xylanase production by a local isolate of *Penicillium janthinellum*. Enzym Microb Technol **15:**248–253. http://dx.doi.org/10.1016/0141-0229(93)90145-R.
30. **Jørgensen H, Mørkeberg A, Krogh KBR, Olsson L.** 2004. Growth and enzyme production by three *Penicillium* species on monosaccharides. J Biotechnol **109:**295–299. http://dx.doi.org/10.1016/j.jbiotec.2003.12.011.
31. **Terrasan CRF, Temer B, Duarte MCT, Carmona EC.** 2010. Production of xylanolytic enzymes by *Penicillium janczewskii*. Bioresour Technol **101:**4139–4143. http://dx.doi.org/10.1016/j.biortech.2010.01.011.
32. **Iembo T, da Silva R, Pagnocca FC, Gomes E.** 2002. Production, characterization, and properties of beta-glucosidase and beta-xylosidase from a strain of *Aureobasidium* sp. Appl Biochem Microbiol **38:**549–552. http://dx.doi.org/10.1023/A:1020774527212.
33. **Knob A, Carmona EC.** 2009. Cell-associated acid beta-xylosidase production by *Penicillium sclerotiorum*. N Biotechnol **26:**60–67. http://dx.doi.org/10.1016/j.nbt.2009.03.002.
34. **Rasmussen LE, Sorensen HR, Vind J, Vikso-Nielsen A.** 2006. Mode of action and properties of the beta-xylosidases from *Talaromyces emersonii* and *Trichoderma reesei*. Biotechnol Bioeng **94:**869–876. http://dx.doi.org/10.1002/bit.20908.
35. **Deshpande N, Wilkins MR, Packer N, Nevalainen H.** 2008. Protein glycosylation pathways in filamentous fungi. Glycobiology **18:**626–637. http://dx.doi.org/10.1093/glycob/cwn044.
36. **Hayes BK, Varki A.** 1993. Biosynthesis of oligosaccharides in intact Golgi preparations from rat liver. Analysis of N-linked glycans labeled by UDP-[6-H-3]galactose, CMP-[9-H-3]N-acetylneuraminic acid, and [acetyl-H-3]acetyl-coenzyme A. J Biol Chem **268:**16155–16169.
37. **Poutanen K, Puls J.** 1988. Characteristics of *Trichoderma reesei* beta-xylosidase and its use in the hydrolysis of solubilized xylans. Appl Microbiol Biotechnol **28:**425–432. http://dx.doi.org/10.1007/BF00268208.
38. **Andrade SD, Polizeli MDLT, Terenzi HF, Jorge JA.** 2004. Effect of carbon source on the biochemical properties of beta-xylosidases produced by *Aspergillus versicolor*. Process Biochem **39:**1931–1938. http://dx.doi.org/10.1016/j.procbio.2003.09.024.
39. **Saha BC.** 2003. Purification and properties of an extracellular beta-xylosidase from a newly isolated *Fusarium proliferatum*. Bioresour Technol **90:**33–38. http://dx.doi.org/10.1016/S0960-8524(03)00098-1.
40. **Bin Y, Hongzhang C.** 2010. Effect of the ash on enzymatic hydrolysis of steam-exploded rice straw. Bioresour Technol **101:**9114–9119. http://dx.doi.org/10.1016/j.biortech.2010.07.033.
41. **Eisenthal R, Danson MJ, Hough DW.** 2007. Catalytic efficiency and k_{cat}/K_m: a useful comparator? Trends Biotechnol **25:**247–249. http://dx.doi.org/10.1016/j.tibtech.2007.03.010.
42. **Xu WZ, Shima Y, Negoro S, Urabe I.** 1991. Sequence and properties of beta-xylosidase from *Bacillus pumilus* Ipo. Contradiction of the previous nucleotide sequence. Eur J Biochem **202:**1197–1203.
43. **Jordan DB, Wagschal K.** 2010. Properties and applications of microbial beta-D-xylosidases featuring the catalytically efficient enzyme from *Selenomonas ruminantium*. Appl Microbiol Biotechnol **86:**1647–1658. http://dx.doi.org/10.1007/s00253-010-2538-y.
44. **Herrmann MC, Vrsanska M, Jurickova M, Hirsch J, Biely P, Kubicek CP.** 1997. The beta-D-xylosidase of *Trichoderma reesei* is a multifunctional beta-D-xylan xylohydrolase. Biochem J **321:**375–381.
45. **Sunna A, Antranikian G.** 1997. Xylanolytic enzymes from fungi and bacteria. Crit Rev Biotechnol **17:**39–67. http://dx.doi.org/10.3109/07388559709146606.
46. **Juturu V, Wu JC.** 2014. Microbial exo-xylanases: a mini review. Appl Biochem Biotechnol **174:**81–92. http://dx.doi.org/10.1007/s12010-014-1042-8.
47. **Dilokpimol A, Nakai H, Gotfredsen CH, Appeldoorn M, Baumann MJ, Nakai N, Schols HA, Abou Hachem M, Svensson B.** 2011. Enzymatic synthesis of beta-xylosyl-oligosaccharides by transxylosylation using two beta-xylosidases of glycoside hydrolase family 3 from *Aspergillus nidulans* FGSC A4. Carbohydr Res **346:**421–429. http://dx.doi.org/10.1016/j.carres.2010.12.010.
48. **Mala S, Dvorakova H, Hrabal R, Kralova B.** 1999. Towards regioselective synthesis of oligosaccharides by use of alpha-glucosidases with different substrate specificity. Carbohydr Res **322:**209–218. http://dx.doi.org/10.1016/S0008-6215(99)00222-0.
49. **Mozolowski G, Connerton I.** 2009. Characterization of a highly efficient heterodimeric xylosidase from *Humicola insolens*. Enzym Microb Technol **45:**436–442. http://dx.doi.org/10.1016/j.enzmictec.2009.08.011.
50. **Kiss T, Kiss L.** 2000. Purification and characterization of an extracellular beta-D-xylosidase from *Aspergillus carbonarius*. World J Microbiol Biotechnol **16:**465–470. http://dx.doi.org/10.1023/A:1008912025896.
51. **Wakiyama M, Yoshihara K, Hayashi S, Ohta K.** 2008. Purification and properties of an extracellular beta-xylosidase from *Aspergillus japonicus* and sequence analysis of the encoding gene. J Biosci Bioeng **106:**398–404. http://dx.doi.org/10.1263/jbb.106.398.
52. **Kumar S, Ramon D.** 1996. Purification and regulation of the synthesis of a beta-xylosidase from *Aspergillus nidulans*. FEMS Microbiol Lett **135:**287–293.
53. **Michelin M, Peixoto-Nogueira SC, Silva TM, Jorge JA, Terenzi HF, Teixeira JA, Polizeli MdL.** 2012. A novel xylan degrading beta-D-xylosidase: purification and biochemical characterization. World J Microbiol Biotechnol **28:**3179–3186. http://dx.doi.org/10.1007/s11274-012-1128-9.
54. **Hayashi S, Ohno T, Ito M, Yokoi H.** 2001. Purification and properties of the cell-associated beta-xylosidase from *Aureobasidium*. J Ind Microbiol Biotechnol **26:**276–279. http://dx.doi.org/10.1038/sj.jim.7000120.
55. **Zanoelo FF, Polizeli MDTD, Terenzi HF, Jorge JA.** 2004. Purification and biochemical properties of a thermostable xylose-tolerant beta-D-xylosidase from *Scytalidium thermophilum*. J Ind Microbiol Biotechnol **31:**170–176. http://dx.doi.org/10.1007/s10295-004-0129-6.
56. **Katapodis P, Nerinckx W, Claeyssens M, Christakopoulos P.** 2006. Purification and characterization of a thermostable intracellular beta-xylosidase from the thermophilic fungus *Sporotrichum thermophile*. Process Biochem **41:**2402–2409. http://dx.doi.org/10.1016/j.procbio.2006.06.021.
57. **Guerfali M, Gargouri A, Belghith H.** 2008. *Talaromyces thermophilus* beta-D-xylosidase: purification, characterization and xylobiose synthesis. Appl Biochem Biotechnol **150:**267–279. http://dx.doi.org/10.1007/s12010-008-8260-x.
58. **Matsuo M, Yasui T.** 1984. Purification and some properties of beta-xylosidase from *Trichoderma viride*. Agric Biol Chem **48:**1845–1852. http://dx.doi.org/10.1271/bbb1961.48.1845.
59. **Jordan DB, Wagschal K, Grigorescu AA, Braker JD.** 2013. Highly active beta-xylosidases of glycoside hydrolase family 43 operating on natural and artificial substrates. Appl Microbiol Biotechnol **97:**4415–4428. http://dx.doi.org/10.1007/s00253-012-4475-4.

60. **Wagschal K, Heng C, Lee CC, Robertson GH, Orts WJ, Wong DW.** Purification and characterization of a glycoside hydrolase family 43 beta-xylosidase from *Geobacillus thermoleovorans* IT-08. Appl Biochem Biotechnol **155:**304–313.
61. **Kirikyali N, Wood J, Connerton IF.** 2014. Characterisation of a recombinant beta-xylosidase (xylA) from *Aspergillus oryzae* expressed in *Pichia pastoris*. AMB Express **4:**68. http://dx.doi.org/10.1186/s13568-014-0068-1.
62. **Kirikyali N, Connerton I.** 2014. Heterologous expression and kinetic characterisation of *Neurospora crassa* beta-xylosidase in *Pichia pastoris*. Enzym Microb Technol **57:**63–68. http://dx.doi.org/10.1016/j.enzmictec.2014.02.002.
63. **Jordan DB.** 2008. Beta-D-xylosidase from *Selenomonas ruminantium*: catalyzed reactions with natural and artificial substrates. Appl Biochem Biotechnol **146:**137–149. http://dx.doi.org/10.1007/s12010-007-8064-4.